

Measurement of Three-Bond ^{13}C – ^{13}C J Couplings between Carbonyl and Carbonyl/Carboxyl Carbons in Isotopically Enriched Proteins

Jin-Shan Hu and Ad Bax*

Laboratory of Chemical Physics
National Institute of Diabetes and
Digestive and Kidney Diseases
National Institutes of Health
Bethesda, Maryland 20892-0520

Received May 15, 1996

Three-bond ^{13}C – ^{13}C J couplings have long been recognized as a valuable source of structural information in the study of organic, organometallic, and biological compounds.^{1–3} For ^{13}C -enriched proteins, two different approaches have been proposed for measurement of these couplings: EASY⁴ and quantitative J correlation.^{5,6} Both approaches benefit from the exceptionally narrow line widths of methyl ^{13}C resonances, and in proteins these measurements therefore have largely been restricted to $^3J_{\text{CC}}$ couplings involving $^{13}\text{CH}_3$. Here we demonstrate that the quantitative J correlation approach can also be used for measurement of $^3J_{\text{CC}}$ couplings between carbonyl (C') and carbonyl/carboxyl carbons. $^3J_{\text{C}'\text{C}'}$ provides direct information on the ϕ backbone angle, and $^3J_{\text{C}'\text{C}'}$ in Asn and Asp residues relates to χ_1 .

Previously, a Karplus curve appropriate for peptides has been proposed on the basis of FPT-INDO calculations.¹ Here we present the first empirical Karplus relation for this coupling based on $^3J_{\text{C}'\text{C}'}$ couplings measured in ubiquitin (76 residues) and ϕ angles from its X-ray structure. Application to apocalmodulin (apo-CaM, 148 residues) confirms the backbone geometry of the first Ca^{2+} -binding site⁷ and adds new information on the orientations of its three Asp side chains which ligate Ca^{2+} in the bound state.

The experiment (Figure 1) for measuring $^3J_{\text{C}'\text{C}'}$ starts with transfer of magnetization from the amide proton (H^{N}) through the ^{15}N to the preceding $^{13}\text{C}'$ and is followed by a $^{13}\text{C}'$ – $^{13}\text{C}'$ dephasing period prior to magnetization transfer to its long-range coupled $^{13}\text{C}'$ which subsequently evolves during t_2 and is finally transferred back along the reverse pathway for $^1\text{H}^{\text{N}}$ detection. The pulse scheme is very similar to that of the long-range carbon–carbon correlation experiment^{5,8} and details regarding the magnetization transfer in this class of experiments have been discussed elsewhere.^{8–10} In the present case, after magnetization has been transferred from ^{15}N to its adjacent $^{13}\text{C}'$ (referred to as source- C' , or sC'), it dephases during the time 2ζ with respect to carbonyls J coupled to sC' . Exactly analogous to the homonuclear HAHA experiment,¹⁰ a fraction

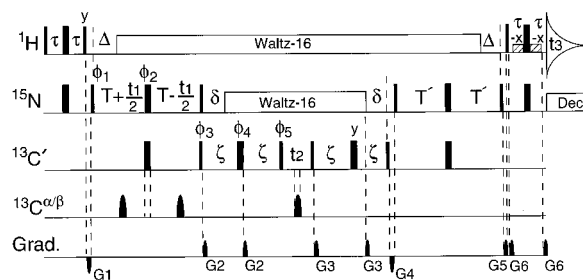


Figure 1. Pulse scheme for the 3D HN(CO)CO experiment. Narrow and wide pulses denote 90° and 180° flip angles (except for low power 90° – x ^1H pulses), respectively, and unless indicated the phase is x . Phase cycling: $\phi_1 = x$; $\phi_2 = 4(x), 4(y), 4(-x), 4(-y)$; $\phi_3 = 2(x), 2(-x)$; $\phi_4 = x$; $\phi_5 = x, -x$; receiver = $2(x), 4(-x), 2(x)$. Quadrature detection in the t_1 dimension is obtained by altering ϕ_1 in the States-TPPI manner, quadrature in t_2 by States-TPPI phase incrementation of ϕ_3, ϕ_4 , and ϕ_5 . RF power: ^1H , $\gamma_{\text{H}}B_1 = 27$ kHz (high-power pulses), 220 Hz (low-power pulses), 3.1 kHz (Waltz-16); ^{15}N , $\gamma_{\text{N}}B_2 = 5.3$ kHz, or 1.0 kHz (Waltz-16); $^{13}\text{C}'$, $\gamma_{\text{C}}B_2 = 4.5$ and 4.0 kHz at 151 and 126 MHz; $^{13}\text{C}^{\alpha/\beta}$, G_3 180° pulses¹⁷ of 400 μs (126 MHz) or 333 μs (151 MHz). Carrier position: ^1H , H_2O (4.79 ppm); $^{13}\text{C}'$, 177 ppm; $^{13}\text{C}^{\alpha/\beta}$, 48 ppm; ^{15}N , 117 ppm. Delay durations: $\tau = 2.5$ ms; $\Delta = 5.3$ ms; $T = 14.5$ ms; $T' = 12.5$ ms; $\delta = 32$ ms; $\zeta = 45$ –55 ms. Gradients (sine bell shaped; 25 G/cm at center): $G_{1,2,3,4,5,6} = 3.75, 0.8, 0.35, 1.65, 1.35, \text{ and } 0.5$ ms.

$\sin(2\pi J_{\text{sC}'\text{dC}'}\zeta) \Pi_{\text{k}} \cos(2\pi J_{\text{sC}'\text{kC}'}\zeta)$ of the source- C' magnetization is transferred to the destination C' , dC' , where the product extends over all C' nuclei, other than dC' , that are J coupled to sC' . A fraction $\cos(2\pi J_{\text{sC}'\text{dC}'}\zeta) \Pi_{\text{k}} \cos(2\pi J_{\text{sC}'\text{kC}'}\zeta)$ remains as in-phase sC' magnetization at the start of t_2 . The same fractions apply to the reverse transfer of C' magnetization between the end of t_2 and the end of the second 2ζ period, and the diagonal-to-cross-peak ratio therefore equals $-\tan^2(2\pi J_{\text{sC}'\text{dC}'}\zeta)$.^{8–10} As ζ is known, $J_{\text{sC}'\text{dC}'}$ follows directly from the intensity ratio. Strictly speaking, this ratio applies to the volume integrals of the sC' and dC' resonances, but as the line widths of the two resonances are identical in the ^{15}N (t_1) and $^1\text{H}^{\text{N}}$ (t_3) dimensions, and the same to within the digital resolution in the C' (t_2) dimension, peak heights are used instead for deriving $J_{\text{sC}'\text{dC}'}$.

Experiments were carried out for samples containing 3.5 mg of $^{13}\text{C}/^{15}\text{N}$ -enriched ubiquitin (pH 4.7; 30 °C) in a 220 μL Shigemi microcell (1.8 mM) at 600 MHz and 10 mg of apo-CaM (pH 6.3; 23 °C) in 450 μL (1.3 mM) at 500 MHz. Experiments on ubiquitin were carried out twice, once with 4 scans (Figure 2A) and once with 16 scans per FID (12 h and 2 d measuring time, respectively). Each strip shows the negative^{9,10} “diagonal” peak, corresponding to the $^{13}\text{C}'$ of the preceding residue, and positive cross peaks to its long-range coupled ^{13}C . For most backbone carbonyls, the value of $^3J_{\text{C}'\text{C}'}$ coupling was measured twice, once with $\text{sC}' = \text{C}'_{i-1}$ and $\text{dC}' = \text{C}'_i$, and once vice versa. The pairwise root-mean-square (rms) difference between these measurements was smaller than 0.1 Hz, and the rms pairwise difference between measured J values in the 4-scan and 16-scan experiments was also less than 0.1 Hz (supporting information). Figure 3 shows the averages of these two measurements as a function of the intervening ϕ angles, taken from the ubiquitin X-ray structure.¹¹ The data were fit to a Karplus curve, yielding

$$^3J_{\text{C}'\text{C}'} = 1.33 \cos^2 \phi - 0.88 \cos \phi + 0.62 \text{ Hz} \quad (1)$$

and a rms difference of 0.18 Hz between measured $^3J_{\text{C}'\text{C}'}$ values and those predicted by eq 1 when using crystallographic ϕ

(1) Bystrov, V. F. *Prog. Nucl. Magn. Reson. Spectrosc.* **1976**, *10*, 41–81.

(2) Marshall, J. L. *Carbon-Carbon and Carbon-Proton NMR Couplings: Applications to Organic Stereochemistry and Conformational Analysis*; VCH: Deerfield Beach, FL, 1983.

(3) Krivdin, L. B.; Della, E. W. *Prog. Nucl. Magn. Reson. Spectrosc.* **1991**, *23*, 301–610.

(4) Schwalbe, H.; Rexroth, A.; Eggenberger, T.; Geppert, T.; Griesinger, C. *J. Am. Chem. Soc.* **1993**, *115*, 7878–7879.

(5) Bax, A.; Max, D.; Zax, D. *J. Am. Chem. Soc.* **1994**, *114*, 6924–6925.

(6) Grzesiek, S.; Vuister, G. W.; Bax, A. *J. Biomol. NMR* **1993**, *3*, 487–493.

(7) Kuboniwa, H.; Tjandra, N.; Grzesiek, S.; Ren, H.; Klee, C. B.; Bax, A. *Nat. Struct. Biol.* **1995**, *2*, 768–776.

(8) Bax, A.; Delaglio, F.; Grzesiek, S.; Vuister, G. W. *J. Biomol. NMR* **1994**, *4*, 787–797.

(9) Cavanagh, J.; Fairbrother, W.; Palmer, A. G., III; Skelton, N. J. *Protein NMR Spectroscopy*; Academic Press: San Diego, CA, 1996; pp 524–528.

(10) Vuister, G. W.; Kim, S.-J.; Wu, C.; Bax, A. *J. Am. Chem. Soc.* **1994**, *116*, 9206–9210.

(11) Vijay-Kumar, S.; Bugg, C. E.; Cook, W. J. *J. Mol. Biol.* **1987**, *194*, 531–544.

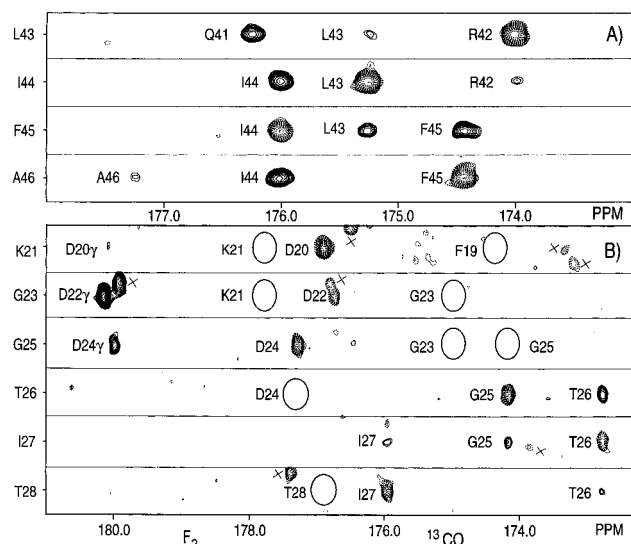


Figure 2. (F_2, F_3) strips from the 3D HN(CO)CO spectra of (A) 1.8 mM ubiquitin (600 MHz, $\zeta = 50$ ms, 4 scans, 12 h), taken at the $^1\text{H}^{\text{N}}$ (F_3) and ^{15}N (F_1) frequencies of Leu⁴³-Ala⁴⁶, and (B) 1.3 mM of apo-CaM (500 MHz, $\zeta = 45$ ms, 12 scans, 48 h), taken at the $^1\text{H}^{\text{N}}/^{15}\text{N}$ frequencies of Lys²¹, Gly²³, Gly²⁵, Thr²⁶, Ile²⁷, and Thr²⁸. The diagonal C' resonance is negative (dashed contours) and corresponds to the C' preceding the amide in the polypeptide. Positions of expected $^3J_{CC'}$ cross peaks, but which are below the noise threshold, are marked by open circles. Correlations from residues with $^1\text{H}^{\text{N}}$ and ^{15}N shifts in the vicinity of the selected amide strip are marked \times . The lower signal-to-noise of the apo-CaM relative to the ubiquitin spectrum results primarily from the nearly 2-fold longer rotational correlation time ($\sim 8^{15}$ vs 4.1 ns), i.e., 2-fold shorter transverse relaxation times.

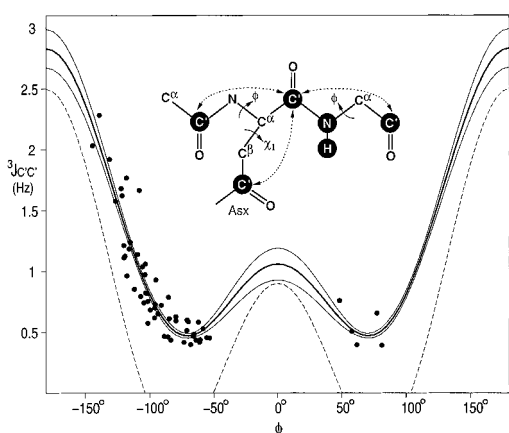


Figure 3. Relation between measured $^3J_{CC'}$ values and crystallographic ϕ angles and a best fit Karplus curve ($^3J_{CC'} = 1.33 \cos^2\phi - 0.88 \cos\phi + 0.62$ Hz). Thin solid lines mark the range of Karplus curves (3 standard deviations) obtained when calculating a set of 10 000 Karplus curves, each time randomly deleting 10% of the data points. The dashed line corresponds to the FPT-INDO parametrization.¹

angles. This difference decreases to 0.16 Hz when using ϕ angles determined on the basis of $^3J_{\text{HNH}\alpha}$, $^3J_{\text{HNC}\beta}$, $^3J_{\text{HNC}'}$, and $^3J_{\text{CH}\alpha}$ couplings,¹² without a significant shift in the Karplus parameters.

$^3J_{CC'}$ couplings measured for Asn and Asp residues range from 0.7 Hz for Asp²⁰ in apo-CaM to 4.5 Hz for Asp²¹ and Asp⁵⁸ in ubiquitin. On the basis of the measurement of $^3J_{\text{H}\alpha\text{H}\beta}$, $^3J_{\text{NH}\beta}$, and $^3J_{\text{CH}\beta}$ for these residues (H. Kuboniwa, J. Marquardt, and A. C. Wang, unpublished results), these values correspond to *gauche* and *trans* couplings, respectively.

At positions 1, 3, and 5 in each of the four 12-residue Ca^{2+} binding sites of CaM are Asp/Asn residues whose γ -carboxyls/carboxyls serve as Ca^{2+} ligands.¹³ In the crystal structure of Ca^{2+} -CaM, the χ_1 angles of these three residues are invariably in the $180^\circ \pm 10^\circ$, $+70^\circ \pm 10^\circ$ and $+75^\circ \pm 10^\circ$ ranges, respectively. In apo-CaM, the backbone of the first half of each Ca^{2+} binding site retains the same conformation,⁷ but in the NMR structure, χ_1 of Asp²² and Asp²⁴ are ill defined. One might expect, however, that the negatively charged side chains repel one another, thereby changing one or more of the χ_1 angles relative to the Ca^{2+} -ligated state. Figure 2B shows (F_2, F_3) strips taken at the ^1H - ^{15}N frequencies of residues K21, G23, G25, T26, I27, and T28. The H^{N} of Lys²¹ shows a very weak cross peak between Asp²⁰- C' and Asp²⁰- $C\gamma$ ($^3J_{CC'\gamma} = 0.7 \pm 0.2$ Hz), in agreement with a dihedral angle of 60° ($\chi_1 = 180^\circ$) in the NMR structure.⁷ Cross peaks to Phe¹⁹- C' and Lys²¹- C' have below-threshold intensity, indicating that the ϕ angles for Asp²⁰ and Lys²¹ must be larger than -100° , in agreement with its solution structure.⁷ The 4.1 Hz $^3J_{CC'\gamma}$ observed for Asp²² is indicative of $\chi_1 \approx -60^\circ$, and $^3J_{CC'\gamma} = 2.2$ Hz for Asp²⁴ suggests rotameric averaging. Thus, upon Ca^{2+} ligation, Asp²⁰ keeps the same χ_1 , Asp²² changes its χ_1 by 120° , and Asp²⁴ changes from flexible to a single rotamer.

Residues Thr²⁶-Thr²⁸ are part of a short antiparallel β -sheet and have ϕ angles of -140° , -140° , and -86° , respectively.⁷ This is confirmed by $^3J_{CC'}$ values of 2.0 (between residues 25 and 26), 1.8 (26 and 27), and <1.2 Hz (27 and 28).

The present report provides the first extensive study of $^3J_{CC}$ couplings between carbonyls. Results indicate that $^3J_{CC'}$ is useful for determining backbone geometry, particularly in combination with $^3J_{\text{HNH}\alpha}$ values, as it removes the ambiguity around $\phi = -120^\circ$ in the $^3J_{\text{HNH}\alpha}$ Karplus curve. Other types of J couplings could also be used for this,^{12,14} but as $^3J_{CC'}$ has its steepest ϕ dependence near $\phi = -120^\circ$ it is particularly well suited for this purpose. Therefore, the HN(CO)CO experiment is a useful addition to the host of recent experiments for determining backbone ϕ angles.^{12,14} Asp and Asn residues frequently play critical roles in intermolecular interactions, and the χ_1 angle information derived from $^3J_{CC'\gamma}$ can be invaluable. The HN(CO)CO experiment is reasonably sensitive and can be carried out in a few days or less. For proteins with relatively long rotational correlation times, such as apo-CaM ($\tau_c \sim 8$ ns),¹⁵ the experiments are best carried out at frequencies of 500 MHz or below, as at higher field strengths the $^{13}\text{C}'$ T_2 , which is dominated by chemical shift anisotropy,¹⁶ decreases rapidly, adversely affecting sensitivity.

Acknowledgment. We thank F. Delaglio and D. Garrett for software, S. Grzesiek, A. C. Wang, J. Marquardt, N. Tjandra, and H. Kuboniwa for help and sharing data on ubiquitin and apo-CaM, and M. Barfield for useful suggestions. This work was supported by the AIDS Targeted Anti-Viral Program of the Office of the Director of the National Institutes of Health. J.-S.H. is supported by a postdoctoral fellowship from the Cancer Research Institute, New York, NY.

Supporting Information Available: One table, containing the $^3J_{CC'}$ couplings measured in human ubiquitin, and one figure showing the correlation between $^3J_{CC'}$ couplings measured from a 4-scan and a 16-scan HN(CO)CO spectrum (4 pages). See any current masthead page for ordering and Internet access instructions.

JA9616239

(13) Babu, Y. S.; Bugg, C. E.; Cook, W. J. *J. Mol. Biol.* **1988**, *204*, 191-204.

(14) Schmidt, J. M.; Löhr, F.; Rüterjans, H. *J. Biomol. NMR* **1996**, *7*, 142-152.

(15) Tjandra, N.; Kuboniwa, H.; Ren, H.; Bax, A. *Eur. J. Biochem.* **1995**, *230*, 1014-1024.

(16) Dayie, K. T.; Wagner, G. *J. Magn. Reson.* **1995**, *109*, 105-108.

(17) Emsley, L.; Bodenhausen, G. *J. Magn. Reson.* **1992**, *97*, 135-148.

(12) Wang, A. C.; Bax, A. *J. Am. Chem. Soc.* **1996**, *118*, 2483-2494.